Lattice dynamics and phonon softening in Ni-Mn-Al Heusler alloys

Xavier Moya, Lluís Mañosa,* and Antoni Planes

*Departament d'Estructura i Constituents de la Matèria, Facultat de Física, Universitat de Barcelona, Diagonal 647,
E-08028 Barcelona, Catalonia, Spain*

Thorsten Krenke and Mehmet Acet

Fachbereich Physik, Experimentalphysik, Universität Duisburg-Essen, D-47048 Duisburg, Germany

V. O. Garlea, T. A. Lograsso, D. L. Schlagel, and J. L. Zarestky

Ames Laboratory, Department of Physics, Iowa State University, Ames, Iowa 50011, USA

Inelastic and elastic neutron scattering have been used to study a single crystal of the $Ni_{54}Mn_{23}Al_{23}$ Heusler alloy over a broad temperature range. The paper reports the experimental determination of the low-lying phonon dispersion curves for this alloy system. We find that the frequencies of the TA_2 modes are relatively low. This branch exhibits an anomaly (dip) at a wave number $\xi_0 = 1/3 \approx 0.33$, which softens with decreasing temperature. Associated with this anomalous dip at ξ_0, an elastic central peak scattering is also present. We have also observed satellites due to the magnetic ordering.

I. INTRODUCTION

Magnetic shape memory behavior is associated with the occurrence of a structural (martensitic) transition in a magnetic material. As a consequence of the degeneracy of the low temperature phase, the martensitic state is a multidomain structure. Rotation of the structural domains due to a difference in Zeeman energy occurs under application of applied magnetic field,[1] thus giving rise to a macroscopic deformation of the sample. Strains as large as 10% have been reported in single crystals of Ni-Mn-Ga.[2,3]

Neutron scattering experiments[4–7] and elastic constant measurements[8–10] have provided evidence of an unusual lattice dynamical behavior in the prototypical magnetic shape memory alloy Ni-Mn-Ga. It has been shown that the transverse TA_2 ($[\xi\xi0]$ direction, $[\xi\bar{\xi}0]$ polarization) branch exhibits a dip (anomalous phonon) at a specific wave number which depends on the particular stacking sequence of the martensite structure. On cooling the energies of the anomalous phonon decrease, and such a phonon softening is enhanced when the sample orders ferromagnetically. For compositions close to the stoichiometric Ni_2MnGa, the energy of the anomalous phonon increases on further cooling below a given temperature T_I, slightly higher than the martensitic transition temperature T_M. Such a change in behavior is associated with a phase transition to the so-called intermediate or premartensitic phase. This transition is driven by a magnetoelastic coupling.[11,12] The temperature behavior of the energy of the anomalous phonon parallels that of the shear elastic constants, which also exhibit a minimum at T_I.[9,10]

The lattice dynamics of Ni-Mn-Ga alloys has been extensively studied from first-principles calculations, and the main experimental features have been successfully reproduced.[13–15] Recently, *ab initio* calculations have been extended to encompass other Heusler alloys.[16–18] Particular effort has been devoted to computing the lattice dynamics of the Ni-Mn-Al system over a broad composition range.[17] For

this system, phonon dispersion curves along the [110] direction have been computed. A complete softening of the TA_2 phonons in the range between $\xi = 0.25$ and $\xi = 0.4$ has been found. The shear elastic constant C' derived from the initial slope of the TA_2 branch has a lower value than the remaining constants.

Up to now, experimental data on phonon dispersion curves and elastic constants in Heusler magnetic shape memory alloys are only available for the Ni-Mn-Ga alloy system. The goal of the present work is to present the experimental determination of the lattice dynamics of Ni-Mn-Al. Although Ni_2MnAl does not transform martensitically, off-stoichiometric alloys transform martensitically within a certain range of compositions close to the stoichiometric one.[19,20] The low temperature martensitic structure depends on composition and the observed structures are the same as those reported for other Ni-Mn based magnetic shape memory alloys.[19–23] The magnetic state of Ni_2MnAl consists of a mixed phase $L2_1 + B2$, which incorporates ferromagnetic and conical antiferromagnetic parts.[24–26] This mixed state is due to the significantly lower $B2 - L2_1$ disorder-order transition temperature, compared to that of Ni-Mn-Ga, which results in very low kinetics for the ordering process.[25] It is also worth mentioning that large magnetic-field-induced strains have been measured on this alloy system.[27]

In this paper, we present elastic and inelastic neutron scattering experiments in a Ni-Mn-Al single crystal. The measured phonon dispersion curves and derived elastic constants are compared to results obtained from *ab initio* calculations.[17] Significant TA_2 phonon softening at $\xi_0 = 0.33$ has been observed. In addition, a number of elastic satellites associated with magnetic ordering and with structural instabilities have been observed.

II. EXPERIMENTAL DETAILS

The single crystal studied was grown by the Bridgman method. Appropriate quantities of nickel (99.99% pure), alu-
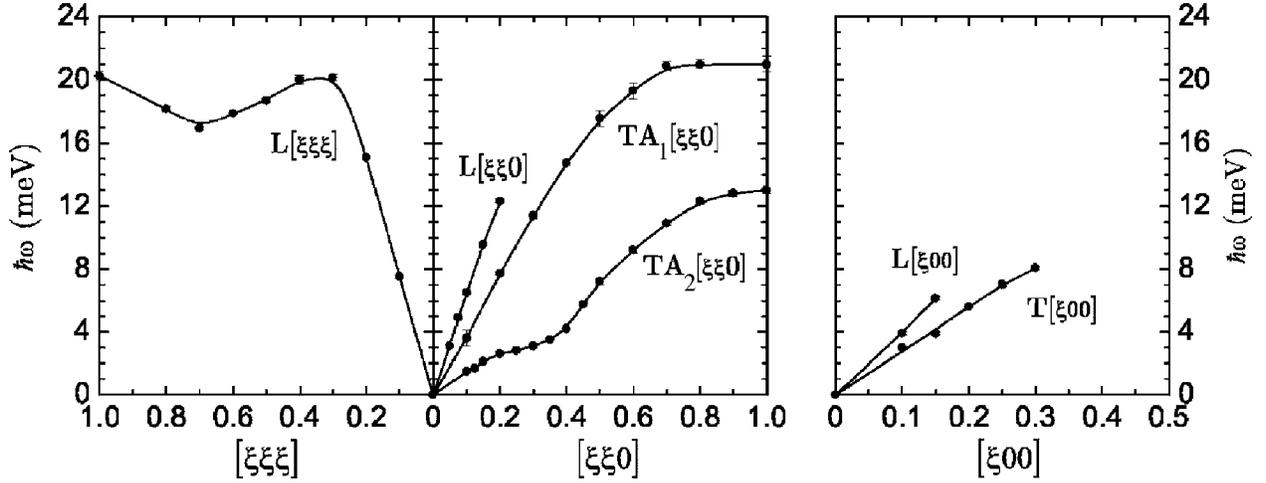
FIG. 1. Acoustic phonon dispersion curves along the high-symmetry directions $[\xi\xi\xi]$, $[\xi\xi0]$, and $[\xi00]$, measured at room temperature. Note the change of the horizontal scale corresponding to the branch measured along the high-symmetry direction $[\xi00]$. Solid lines are guides to the eye.

minum (99.99%), and electrolytic manganese (99.9%) were cleaned and arc melted several times under an argon atmosphere. The nominal composition of the alloy was $Ni_{50}Mn_{25}Al_{25}$. The button was then remelted and the alloy drop cast into a copper chill cast mold to ensure compositional homogeneity throughout the ingot. The as-cast ingot was placed in alumina crucibles (approximately 15 mm in diameter) and crystal growth was done in a Bridgman-style refractory metal resistance furnace. The ingot was heated to 1350 °C for 1 h to allow homogenization before withdrawing the sample from the heat zone at a rate of 5.0 mm/h. To minimize vaporization of the manganese during crystal growth, the furnace was backfilled to a positive pressure of 6.8×10^5 Pa with purified argon after the chamber and sample had been out gassed at 1350 °C under vacuum. The average composition of the alloy was determined by energy dispersive x-ray photoluminescence analysis (EDX) to be $Ni_{54}Mn_{23}Al_{23}$ (within ±1 at. %).

Small pieces cut from the top and bottom of the ingot using a low speed diamond saw were used as samples for magnetization and calorimetric studies in order to characterize the sample. Both magnetization and calorimetric studies revealed a magnetic transition at $T \simeq 300$ K. Similar behavior was observed in polycrystalline samples with composition close to the studied sample.[25]

Neutron scattering measurements were carried out on the HB1A (Ames Laboratory PRT) spectrometer at the high flux isotope reactor (HFIR) of the Oak Ridge National Laboratory. The monochromator and analyzer used the (002) reflection of pyrolitic graphite (PG) and highly oriented PG filters (HOPG) were used to minimize higher-order contaminations of the beam. The HB1A spectrometer operates at a fixed incident energy of 14.6 meV which requires that scans with energy transfers over ~9 meV be performed using neutron-energy gain. However, much of the low energy (low-q) range of each branch was measured using the higher resolution neutron-energy loss mode. Collimations of 48′-40′-40′-136′ were used and all scans were performed in the constant-Q mode while counting against neutron monitor counts. Two

sample settings were used. The sample was aligned to have either the (001) or the (1$\bar{1}$0) planes coincide with the scattering plane of the spectrometer.

A standard closed-cycle helium refrigerator (displex) was used for measurements below room temperature and up to 350 K. The sample was mounted under helium atmosphere in an aluminum sample container attached to the cold finger of the displex. The high temperature measurements (623 K) were performed with the sample mounted in a 10^{-5} Torr vacuum furnace.

III. EXPERIMENTAL RESULTS AND DISCUSSION

A. Phonon dispersion

Phonon dispersion curves were determined from inelastic neutron scattering along the high-symmetry directions $[\xi00]$, $[\xi\xi0]$, and $[\xi\xi\xi]$. The room temperature results are shown in Fig. 1. Note that the dispersion curves are plotted in an extended Brillouin zone scheme in the fcc $L2_1$ notation, (lattice parameter $a = 5.82$ Å). The phonon spectrum found for the studied system shows the features typical of bcc materials:[28] (i) low energies of the phonons in the $TA_2[\xi\xi0]$ branch, and (ii) the marked dip at $\xi = 2/3$ in the longitudinal $L[\xi\xi\xi]$ branch. The dip in the $L[\xi\xi\xi]$ branch is related to the incipient instability towards the so-called ω phase. The most noteworthy feature is the wiggle at $\xi_0 \approx 0.33$ in the $TA_2[\xi\xi0]$

TABLE I. Elastic constants obtained from the initial slopes of the acoustic phonon branches at $\xi \rightarrow 0$ at room temperature. The calculated values, corresponding to the stoichiometric Ni_2MnAl sample, are extracted from Ref. 17.

	Measured value (GPa)	Calculated value (GPa)
C_{44}	103±5	102
C_L	259±5	263
C'	16±5	32
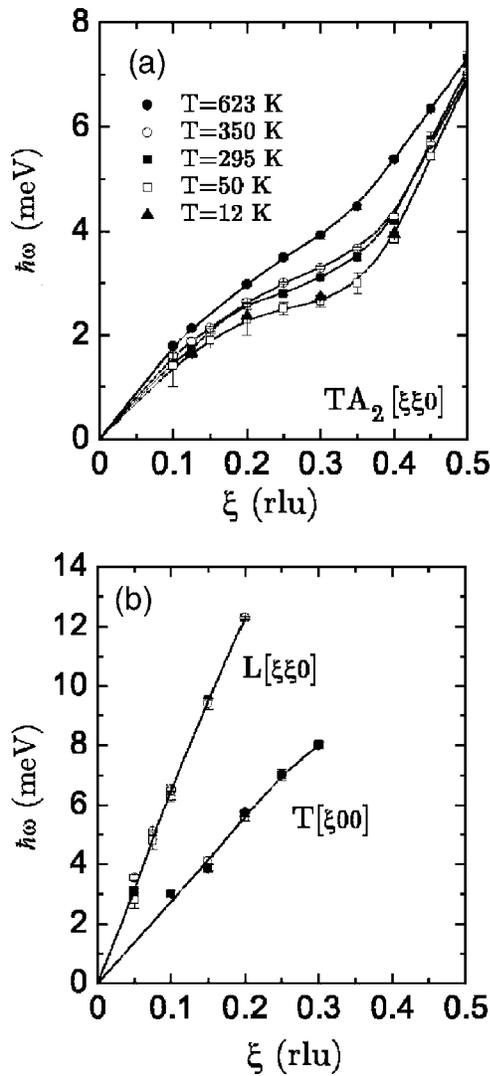
FIG. 2. Temperature dependence of the partial acoustic dispersion curves. (a) Temperature dependence of the anomaly in the $TA_2[\xi\xi0]$ branch. (b) Temperature dependence of the longitudinal $L[\xi\xi0]$ and transverse $T[\xi00]$. Whereas the wiggle at $\xi_0 \approx 0.33$ in the $TA_2[\xi\xi0]$ branch deepens with decreasing temperature, the other measured branches do not change significantly. Solid lines are guides to the eye.

branch, which deepens strongly with decreasing temperature, as shown in Fig. 2(a). A similar behavior has also been reported for Ni-Mn-Ga alloys with composition close to the stoichiometric Ni_2MnGa.[4,7] According to recent *ab initio* calculations,[17] such a phonon softening is due to a strong electron-phonon coupling and the Kohn anomaly.

The temperature dependent softening of the $\xi_0 \approx 0.33$ TA_2 phonon is illustrated in Fig. 3, which shows the energy squared of the soft phonon as a function of temperature. For comparison, data for the soft phonons in Ni_2MnGa and $Ni_{62.5}Al_{37.5}$ alloys are also plotted. The degree of softening is similar to that of $Ni_{62.5}Al_{37.5}$, although the actual energy values are higher which is consistent with the fact that the studied sample does not transform martensitically within the studied temperature range. The softening in Ni_2MnGa is stronger due to strong spin-phonon coupling in the ferromag-
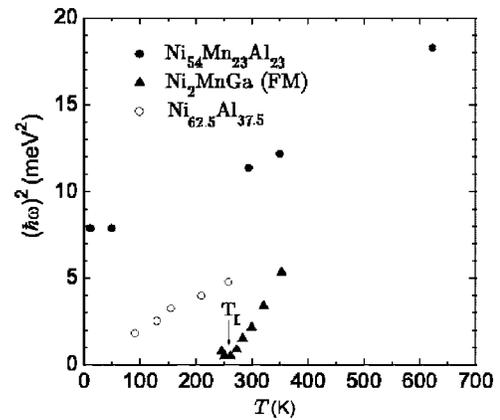
FIG. 3. Temperature dependence of the energy squared of the $TA_2[\xi\xi0]$ $\xi_0=0.33$ phonon. Data from related systems Ni_2MnGa and $Ni_{62.5}Al_{37.5}$ are also shown for comparison. T_I represents the premartensitic transformation temperature. The data for the latter systems were taken from Refs. 5 and 29 for Ni_2MnGa and $Ni_{62.5}Al_{37.5}$, respectively.
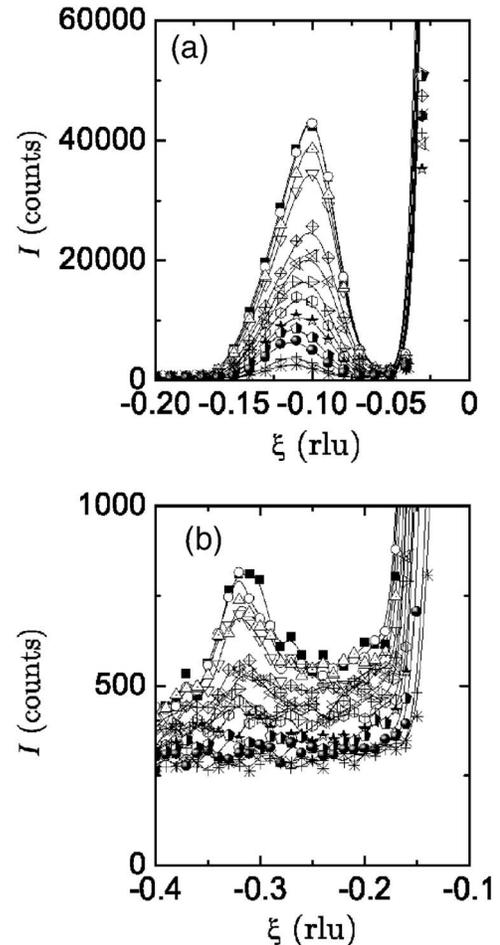
FIG. 4. Temperature dependence of the elastic scattering along the $[\bar{\xi}\xi0]$ direction starting from the (020) reflection. (a) Satellite due to the conical antiferromagnetic order. (b) Central peak associated with the anomalous dip at ξ_0 in the acoustic $TA_2[\xi\xi0]$ phonon branch. Temperatures from top to bottom are 12, 50, 75, 100, 150, 175, 200, 225, 250, 275, 300, 330, and 350 K. Solid lines are guides to the eye.
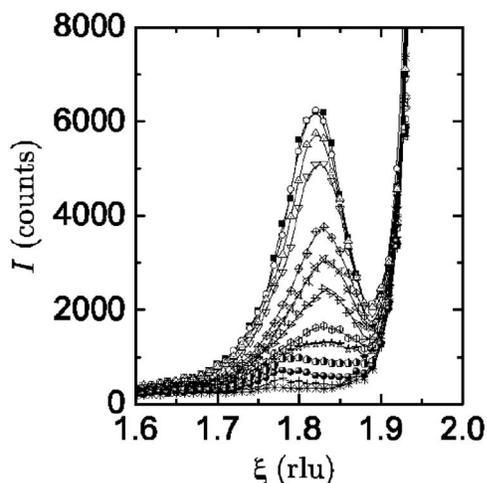
FIG. 5. Temperature dependence of the elastic scattering along the $[\bar{\xi}\xi 0]$ direction starting from the (220) reflection. Temperatures from top to bottom are 12, 50, 75, 100, 150, 175, 200, 225, 250, 275, 300, 330, and 350 K. Solid lines are guides to the eye.

netic state. It must be noted that the phonon branches other than the TA_2 do not change significantly with temperature as can be seen from Fig. 2(b).

The measured dispersion curves are in good agreement with those obtained from *ab initio* calculations for the [110] direction of the stoichiometric Ni_2MnAl.[17,18] The energies of the acoustic phonons coincide within the errors except for the low energy transverse TA_2 branch, which exhibits complete softening in the range between $\xi=0.25$ and $\xi=0.4$. Experimental data are in agreement with such an instability and show that the minimum is located at $\xi_0 \simeq 0.33$. However, from Fig. 2(a), it can be seen that the softening is not complete, i.e., the phonon frequency remains finite even at the lowest temperatures.

The elastic constants at room temperature obtained from the initial slopes of the acoustic phonon branches at $\xi \rightarrow 0$ are summarized in Table I. First-principles calculations of lattice dynamics have provided theoretical values at 0 K for the elastic constants of the stoichiometric Ni_2MnAl compound.[17] The measured and the calculated values are in good agreement, except for C' which corresponds to the initial slope of the TA_2 branch. The value obtained from the measured curve is lower than that obtained from the calculated one. While it is not expected that C_L and C_{44} strongly depend on composition, C' may change from one composition to another. In addition, it is worth noticing that the value is affected by a large error due to the difficulty in defining the initial slope of the curve.

B. Quasielastic scattering

As previously reported in other related systems,[4] diffuse quasielastic scattering exists associated with the phonon anomalies on the low-lying branch. A satellite peak—the *central peak*—develops at the wave vector which corresponds to the position of the dip in the $TA_2[\xi\xi 0]$ branch. Figure 4 shows the temperature dependence of the elastic scattering along $[\bar{\xi}\xi 0]$ direction starting from the (020) re-
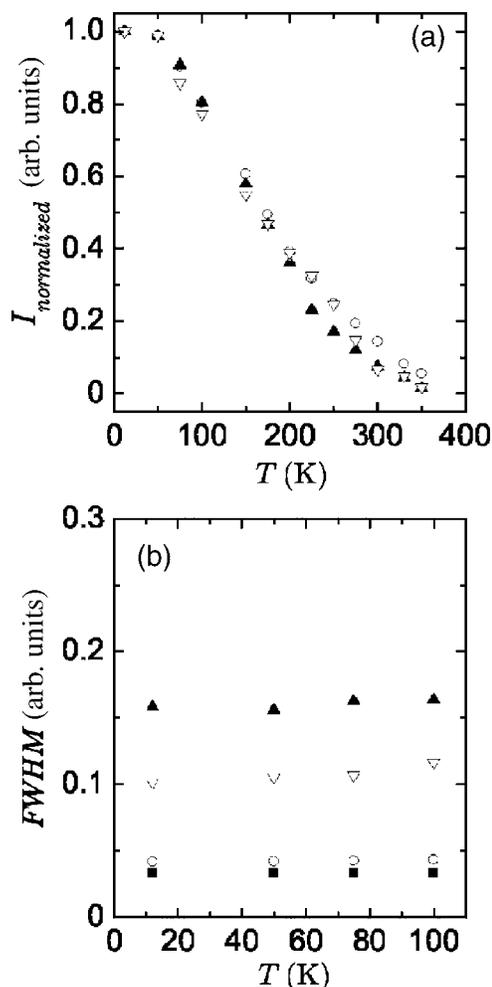
FIG. 6. Temperature dependence of (a) normalized maximum intensity, and (b) width (FWHM) of the elastic satellites reported. Symbols $\bigcirc$, $\blacktriangle$, and ∇ represent the $[-0.1, 2.1, 0]$, $[1.82, 2.18, 0]$, and $[-0.33, 2.33, 0]$ satellites, respectively. The width of the (020) Bragg reflection ($\blacksquare$) is also shown in order to compare the widths of the satellites to the fundamental reflections. None of the widths of the Bragg peaks measured were instrumentally limited.

flection. From this figure, we can distinguish two different elastic satellites in addition to the Bragg peak at $\xi=0$. The first satellite [Fig. 4(a)], at $\xi \approx 0.1$, is due to the conical antiferromagnetic order as determined by Ziebeck and Webster.[26] The second satellite [Fig. 4(b)], at $\xi \approx 0.33$, is a central peak associated with the anomalous dip at ξ_0 in the acoustic $TA_2[\xi\xi 0]$ phonon branch.

We have also measured elastic scattering along $[\bar{\xi}\xi 0]$ direction starting from the fundamental reflection (220). Results are shown in Fig. 5. A satellite located at $\xi \approx 0.18$ is observed. Such a satellite was also reported in Ni_2MnGa from x-ray[30] and neutron scattering[6] experiments, and it was attributed to the splitting of the Bragg peak owing to a tetragonal phase distortion.

Figure 6(a) shows the temperature dependence of the maximum intensity of the observed satellites normalized to the value at $T=12$ K. Figure 6(b) shows the temperature dependence of the full width at half maximum (FWHM) of the different satellites compared to that of the (020) Bragg re-

flection. The satellite corresponding to the conical antiferromagnetic order has similar width compared to the Bragg reflections, whereas the other two reported satellites have less intensity (see Figs. 4 and 5) and are broader in q space than the lattice reflections.

From the similarity in the temperature dependence of the $\xi \approx 0.18$ and $\xi \approx 0.33$ satellites, Stuhr *et al.*[6] concluded that they were caused by dynamic precursor effects rather than (static) contributions of the low temperature phase. Our data for Ni-Mn-Al also show a similar temperature dependence for these two satellites and therefore the origin could be the same than in Ni-Mn-Ga: the $\xi \approx 0.18$ being a precursor of the tetragonal deformation and the $\xi \approx 0.33$, a precursor of the martensite modulation. It must be noted, however, that although the $\xi \approx 0.33$ satellite has been observed in all the investigated Ni-Mn-Ga samples, the one at $\xi \approx 0.18$ has not always been observed. It seems that the appearance of such a satellite can be sample dependent and it might be related to the homogeneity of the sample under study. This is consistent with the fact that the martensitic transition temperature in these alloy systems is extremely sensitive on composition, and therefore the existence of a small amount of martensite growing as temperature decreases cannot be completely disregarded.

Figures 4–6 show that precursor satellites only grow once the sample orders magnetically. Again, this situation parallels the behavior observed in Ni-Mn-Ga. For that alloy system satellites also grow below the Curie point.[6] Moreover, for that alloy system, an enhancement of the phonon softening occurs in the ferromagnetic phase.[6,7] Hence, present results suggest that in Ni-Mn-Al the development of magnetic order also affects lattice stability.

IV. SUMMARY AND CONCLUSIONS

We have measured the low-lying phonon dispersion curves of a $Ni_{54}Mn_{23}Al_{23}$ alloy. We found that the frequencies of the $TA_2[\xi\xi0]$ modes are relatively low, thus evidencing a low dynamical stability for distortions on the $\{110\}$ planes along the $\langle 1\bar{1}0 \rangle$ directions. This branch has an anomaly (dip) at a wave vector $\xi_0 = 1/3 \approx 0.33$. The energy of this phonon decreases with decreasing temperature. The existence of this anomaly in the phonon branch was predicted from recent *ab initio* calculations. Associated with this anomalous dip at ξ_0, an elastic central peak scattering is also present. The reported behavior is similar to that observed in the related Ni-Mn-Ga system but with a less softening of the TA_2 phonon in Ni-Mn-Al. Overall, the energies of the acoustic TA_2 branch show higher values compared to those in Ni-Mn-Ga. This is consistent with the fact that the studied crystal does not transform martensitically within the studied temperature range.

*Electronic address: lluis@ecm.ub.es

[1] R. C. O'Handley, J. Appl. Phys. **83**, 3263 (1998).

[2] K. Ullakko, J. K. Huang, C. Kanter, R. C. O'Handley, and V. V. Kokorin, Appl. Phys. Lett. **69**, 1966 (1996).

[3] A. Sozinov, A. A. Likhachev, N. Lanska, and K. Ullakko, Appl. Phys. Lett. **80**, 1746 (2002).

[4] A. Zheludev, S. M. Shapiro, P. Wochner, A. Schwartz, M. Wall, and L. E. Tanner, Phys. Rev. B **51**, 11310 (1995).

[5] A. Zheludev, S. M. Shapiro, P. Wochner, and L. E. Tanner, Phys. Rev. B **54**, 15045 (1996).

[6] U. Stuhr, P. Vorderwisch, V. V. Kokorin, and P.-A. Lindgård, Phys. Rev. B **56**, 14360 (1997).

[7] L. Mañosa, A. Planes, J. Zarestky, T. Lograsso, D. L. Schlagel, and C. Stassis, Phys. Rev. B **64**, 024305 (2001).

[8] J. Worgull, E. Petti, and J. Trivisonno, Phys. Rev. B **54**, 15695 (1996).

[9] L. Mañosa, A. Gonzàlez-Comas, E. Obradó, A. Planes, V. A. Chernenko, V. V. Kokorin, and E. Cesari, Phys. Rev. B **55**, 11068 (1997).

[10] M. Stipcich, L. Mañosa, A. Planes, M. Morin, J. Zarestky, T. Lograsso, and C. Stassis, Phys. Rev. B **70**, 054115 (2004).

[11] A. Planes, E. Obradó, A. Gonzàlez-Comas, and L. Mañosa, Phys. Rev. Lett. **79**, 3926 (1997).

[12] T. Castán, E. Vives, and P.-A. Lindgård, Phys. Rev. B **60**, 7071 (1999).

[13] Y. Lee, J. Y. Rhee, and B. N. Harmon, Phys. Rev. B **66**, 054424 (2002).

[14] A. T. Zayak, P. Entel, J. Enkovaara, A. Ayuela, and R. M. Nieminen, Phys. Rev. B **68**, 132402 (2003).

[15] C. Bungaro, K. M. Rabe, and A. Dal Corso, Phys. Rev. B **68**, 134104 (2003).

[16] J. Enkovaara, A. Ayuela, J. Jalkanen, L. Nordström, and R. M. Nieminen, Phys. Rev. B **67**, 054417 (2003).

[17] T. Büsgen, J. Feydt, R. Hassdorf, S. Thienhaus, M. Moske, M. Boese, A. Zayak, and P. Entel, Phys. Rev. B **70**, 014111 (2004).

[18] A. T. Zayak, P. Entel, K. M. Rabe, W. A. Adeagbo, and M. Acet, Phys. Rev. B **72**, 054113 (2005).

[19] R. Kainuma, H. Nakano, and K. Ishida, Metall. Mater. Trans. A **27A**, 4153 (1996).

[20] A. Morito, T. Kakeshita, K. Hirata, and K. Otsuka, Acta Mater. **46**, 5377 (1998).

[21] S. Morito, and K. Otsuka, Mater. Sci. Eng., A **208**, 47 (1996).

[22] J. Pons, V. A. Chernenko, R. Santamarta, and E. Cesari, Acta Mater. **48**, 3027 (2000).

[23] T. Krenke, M. Acet, E. F. Wassermann, X. Moya, L. Mañosa, and A. Planes, Phys. Rev. B **72**, 014412 (2005).

[24] M. Acet, E. Duman, E. F. Wassermann, L. Mañosa, and A. Planes, J. Appl. Phys. **92**, 3867 (2002).

[25] L. Mañosa, A. Planes, M. Acet, E. Duman, and E. F. Wassermann, J. Appl. Phys. **93**, 8498 (2003).

[26] K. R. A. Ziebeck, and P. J. Webster, J. Phys. F: Met. Phys. **5**, 1756 (1975).

[27] A. Fujita, K. Fukamichi, F. Gejima, R. Kainuma, and K. Ishida, Appl. Phys. Lett. **77**, 3054 (2000).

[28] A. Planes and L. Mañosa, Solid State Phys. **55**, 159 (2001).

[29] S. M. Shapiro, B. X. Yang, Y. Noda, L. E. Tanner, and D. Schryvers, Phys. Rev. B **44**, 9301 (1991).

[30] G. Fritsch, V. V. Kokorin, and A. Kempf, J. Phys.: Condens. Matter **6**, L107 (1994).